Investigation of the sub-Neptune photoevaporation desert for M-dwarfs to Sun-like stars

Kavli Summer Program in Astrophysics 2016: Exoplanetary Atmospheres

George D. McDonald*[1], Laura Kreidberg[2], and Eric Lopez[3]

[1] *School of Earth & Atmospheric Sciences, Georgia Institute of Technology, Atlanta GA*

[2] *Institute for Theory & Computation, Harvard-Smithsonian Center for Astrophysics, Boston MA*

[3] *Institute for Astronomy, The Royal Observatory, Edinburgh UK*

September 1, 2016

Abstract: Short-period sub-Neptunes with substantial volatile envelopes are among the most common type of known exoplanets. However, these planets are typically on highly-irradiated orbits where they are vulnerable to atmospheric photoevaporation. In particular, recent studies of the *Kepler* planet population have suggested a dearth of sub-Neptunes on orbits receiving more than 650× the broadband irradiation of the Earth (Lundkvist et al. 2016). Physically, we expect this "photoevaporation desert" to depend on the lifetime integrated X-ray and extreme ultraviolet flux, which is the main driver of atmospheric escape for these planets. In this work, we compute planet occurrence as a function of integrated X-ray flux for the latest samples of confirmed *Kepler* and *K2* planets. Our objective is to constrain the desert in a parameter space that ties directly to the photoevaporation process. We find a sharp drop-off in planet occurrence for integrated X-ray flux

*Corresponding author, `gdmcdonald@gatech.edu`

greater than 4×10^{21} erg/cm^2, and we also investigate how this drop-off varies with stellar spectral type.

1 Introduction

The *Kepler* mission has confirmed over 2268 extrasolar planets (Morton et al., 2016). These discoveries provide valuable information about the distribution of planets in terms of planetary radius and semi-major axis. Of particular significance has been the discovery that given the curent sample of close-in planets (5-50 day periods), the most common type are planets with radii of $2 - 2.8$ $R_\oplus$ (Earth radii), hereafter refered to as sub-Neptunes (Fressin et al., 2013; Petigura et al., 2013).

Studies of the mass-radius relations of these planets indicate that they are a diverse population, spanning bulk densities consistent with compositions of pure rock to pure water, and finally those whose densities are low enough that they require hydrogen/helium envelopes (Weiss et al., 2013; Lopez and Fortney, 2014). While there is good evidence that planets with $R_\oplus \geq 1.6$ are not purely rocky (Rogers, 2015), many open questions remain, particularly with respect to the diversity of the compositions of the planets that do have envelopes. It is important to not only place constraints on the present-day compositions of these planets, but to also recognize that the observed densities are snapshots in time, and that an evolution across these different compositions is probable for many sub-Neptunes.

Specifically, for sub-Neptunes around sun-like stars with orbital periods $\lesssim 10$ days, photoevaporation has been suggested as a mechanism for stripping these planets of their hydrogen/helium envelopes (Owen and Jackson, 2012). This would result in an enrichment in metals and a reduction in the radii of these planets. The mechanism of this photoevaporation process involves the photoionization of hydrogen due to the absorption of X-ray and extreme ultraviolet radiation (XUV). This process occurs at atmospheric pressures of around a nanobar, where the atmosphere becomes opaque to the XUV (Murray-clay et al., 2009). The thermal excitation resulting from the photoionization produces a hydrodynamic escape of the atmospheric hydrogen/helium.

Evolution models of sub-Neptunes, which account for the effects of hydrodynamic mass-loss and thermal contraction, have been developed to study photoevaporation-driven atmospheric escape. Studies that have run these models over large parameter spaces in incident bolometric flux and planetary mass have indicated a threshold above which planets will not be found after > 100 Myr due to photoevaporation-driven mass loss (Lopez et al., 2012; Owen and Wu, 2013). The thresholds produced by these models are in good agreement with observations in terms of acting as bounds for a region where there is a dearth of observed planets (Lopez et al., 2012; Lopez and Fortney, 2014).

Nevertheless, the sample of planets for which masses (and bulk densities) are known is relatively small. This has motivated searches for regions with a lack of sub-Neptune sized planets in the *Kepler* dataset, where masses for most planets are unknown, but planetary radii have been measured. These searches are carried out in the parameter space of planetary radius and incident bolometric flux. Sanchis-Ojeda et al. 2014 examined the population of *Kepler* planets with orbital periods less than one day, and noted a lack of planets larger than 2 $R_{\oplus}$, suggesting that photoevaporation could be responsible for this observation. More recently, Lundkvist et al. 2016 used a sample of planets around host stars with asteroseismic observations to suggest a lack of planets with bolometric fluxes greater than 650 times the solar constant (650 $F_{\oplus}$) and radii between 2.2 and 3.8 $R_{\oplus}$.

The mounting evidence for a "photoevaporation desert," or a dearth of sub-Neptunes on close-in orbits, in the *Kepler* data is intriguing. However, many open questions remain that need to be answered in order to maximize the information about the evolution of sub-Neptunes that can be gleaned from the data. Firstly, the current constraints on the photoevaporation desert arise from a relatively small sample of 157 planets whose host stars have asteroseismic measurements. Furthermore, one expects the photoevaporation desert to depend on the lifetime integrated XUV flux, which is the main driver of atmospheric escape for these planets, and not on the present-day bolometric flux. Finally, the recent rapid increase in the number of known exoplanets, specifically the 1284 new confirmed planets by the uniform false positive probability analysis of Morton et al. 2016, and the 104 first confirmed planets by *Kepler*'s *K2* mission (Crossfield et al., 2016), present an opportunity for placing more stringent constraints on the desert's boundaries. With a sample size greater than 2350 planets, it is also possible to see how the desert varies as a function of the host star's spectral type.

We examine how lifetime-integrated X-ray fluxes vary as a function of stellar spectral type, using the X-ray flux evolution tracks reported from observations by Jackson et al. 2012 and Shkolnik and Barman 2014. We then calculate lifetime-integrated X-ray fluxes for the full *Kepler* sample and examine the photoevaporation desert in this parameter space. We find that sub-Neptunes become exceedingly rare for integrated X-ray fluxes greater than 4×10^{21} erg/cm^2. We also examine how the photoevaporation desert varies as a function of stellar spectral type. Our ultimate goal is to calculate occurence rates in the planetary radii vs lifetime-integrated X-ray flux parameter space, for both the *Kepler* and *K2* samples.

2 Methods

2.1 X-ray evolution

To track the evolution of X-ray flux as a function of time for different stellar spectral types, we use the observationally derived relations in Jackson et al. 2012 and Shkolnik and Barman 2014. Jackson et al. 2012 use X-ray survey observations of open clusters to report the ratio of the X-ray to bolometric luminosity over stellar ages of 10 Myr to 4.5 Gyr, with bins spanning stellar spectral types from K5 to F0. Shkolnik and Barman 2014 use ROSAT (Röntgensatellit) observations to determine the X-ray to J-band (centered at 1.25 μm) flux from stellar ages of 10 Myr to 5 Gyr for M4 to K4 spectral types.

The same trend of a saturated phase of X-ray emission early in the lifetime of the star (tens to hundreds of millions years) followed by a power-law decay is found across all stellar spectral types **(Fig. 1)**. The difference between spectral types is that as stellar mass decreases, stars saturate with a greater proportion of their luminosity in the X-rays, while the saturation phase also increases in duration (Jackson et al., 2012; Shkolnik and Barman, 2014). Both trends are visible in **Fig. 1**. This behavior is not monotonic across spectral types as a result of the uncertainties in the observations—nevertheless the overall trend is apparent.

With the exception of the sun, extreme ultraviolet (EUV, 10-124 nm) observations of stars are scarce. Thus, while studies have used models derived from solar observations to estimate EUV fluxes for old, sun-type stars (Lecavelier Des Etangs, 2007; Sanz-Forcada et al., 2011), such extrapolations are not possible for other stellar types. Thus, we focus specifically on the evolution of the X-rays. X-rays are the primary driver for hydrodynamic escape (Owen and Jackson, 2012). Furthermore, the EUV emission for sun-type stars (Sanz-Forcada et al., 2011), and the trends of the near and far ultraviolet for M-dwarfs (Shkolnik and Barman, 2014), are all suggestive that the EUV evolution qualitatively follows the same saturation and decay behavior as the X-rays.

2.2 Calculating lifetime-integrated X-ray flux

Our interest is in calculating the lifetime-integrated X-ray flux for the full *Kepler* sample. We first need a way of classifying a star's spectral type; we use stellar mass from the *Kepler* Q1-17 DR 24 Stellar catalog, which has been calculated for all *Kepler* stars by comparing available observations (which differ among the *Kepler* host stars—spectroscopic, asteroseismic, photometric observations etc.) with the Dartmouth Stellar Evolution Database isochrones (Dotter et al., 2008; Huber et al., 2014).

However, the Jackson et al. 2012 X-ray to bolometric luminosity ratio evolution tracks are binned by stellar spectral type in the form of B-V color (magnitude in the B band, centered at 445 nm, minus magnitude in the V band, centered at 551 nm. B-V color is not a standard *Kepler* measurement), rather than mass. Thus, a method for converting the *Kepler* Stellar catalog masses to a B-V color is required. We use the Pecaut and Mamajek 2013 mean dwarf sequence to convert present-day stellar masses to B-V colors. Furthermore, because the Jackson et al. 2012 and Shkolnik and Barman 2014 relations describe the ratio of the X-ray luminosity to either the bolometric or

J-band luminosity, we need information on the bolometric or J-band luminosity evolution for the stars of interest. This information is provided by the Baraffe et al. 1998 stellar evolution models.

Now the X-ray luminosity as a function of stellar age can be determined for stars of any given mass between 0.3 and 1.598 $M_{\odot}$ (the bounds of the Jackson et al. 2012 and Shkolnik and Barman 2014 measurements); what remains is to integrate the X-ray luminosity over the lifetime of a given star. This lifetime-integrated X-ray luminosity is then converted to a flux at the semi-major axis of the planet of interest, as it is this lifetime-integrated X-ray flux that will control photoevaporation. Because the majority of *Kepler* stars do not have age constraints, we assume ages of 5 Gyr for the full *Kepler* sample. The small sample of *Kepler* stars with age estimates from asteroseismic measurements indicate ages greater than that of the Sun (Silva Aguirre et al., 2015), noting however that the stars with asteroseismic measurements are not representative of the whole *Kepler* sample. Despite the lack of age constraints for most *Kepler* stars, it is important to consider that the X-ray luminosity of all stellar types is controlled primarily by the output of the first several hundred million years (the saturation phase). Thus, changing the assumption of a star's age from 5 Gyr to 2 Gyr only introduces a factor of ~ 2 change in the calculated lifetime-integrated X-ray flux.

2.3 Application to the *Kepler* sample

We calculate the lifetime-integrated X-ray fluxes for the full *Kepler* sample using the method described in section 2.2. The specific sample that we use is the *Kepler* Q1-Q17 DR 24 *Kepler* Object of Interest (KOI) table, specifically the sample of 2268 planets confirmed with the uniform false-positive probability analysis of Morton et al. 2016.

3 Results

3.1 Lifetime-integrated X-ray flux as a function of stellar mass

We first present the variation in lifetime-integrated X-ray flux as a function of stellar mass, for a planet with a semi-major axis of 0.01 AU **(Fig. 2)**. The lifetime-integrated X-ray flux increases as the stellar mass increases, which is not surprising given that the bolometric luminosity increases with mass. What is not quite as intuitive, is that the lifetime-integrated X-ray flux changes by only an order of magnitude for stars with $0.3 < M_{\odot} < 1.598$, despite the fact that the bolometric luminosity varies by two orders of magnitude over this mass range. This is a result of competition between the bolometric luminosity increase with increasing stellar mass and the decrease in the proportion of the bolometric luminosity emitted in X-rays with increasing stellar mass (as in **Fig. 1**). The *Kepler* stars range in spectral type from M to A-dwarfs, thus the lifetime-integrated X-ray flux for a given planet will depend not only on its distance from its host star, but also on the spectral type of the star.

3.2 The *Kepler* planets in lifetime-integrated X-ray flux parameter space

We first present the confirmed *Kepler* planets in the familiar parameter space of planet radius vs. present-day bolometric flux at the planet's semi-major axis **(Fig. 3)**. This is the same presentation of the *Kepler* data as that in Lundkvist et al. 2016, with the exception that we are showing the planets confirmed by the Morton et al. 2016 analysis (adding 1284 planets) and making no cuts to the sample based on measurement precision. The photoevaporation desert reported by Lundkvist et al. 2016 is the rectangular region with a bolometric flux > 650 $F_{\oplus}$ and radii between 2.2 and 3.8 $R_{\oplus}$. Without making cuts to the *Kepler* data based on measurement precision, planets appear in the desert.

We now show the confirmed *Kepler* planets after our calculation of lifetime-integrated X-ray flux for the full sample in **Fig. 4**. Of interest is the formation of cleaner bounds to the desert region in this parameter space. In particular, placing a boundary at 4×10^{21} erg/cm^2 and 2.2 and 4 $R_\oplus$ leaves only one planet in the desert region (K06527.01, the planet does not yet have a *Kepler* designation because it was confirmed by the uniform false-positive probability analysis of Morton et al. 2016). This stands in contrast with the > 20 planets that appear in the desert in the present-day bolometric flux space of **Fig. 3**.

3.3 The photoevaporation desert as a function of stellar type and the calculation of occurence rates

The desert region in the lifetime-integrated X-ray flux parameter space as a function of stellar spectral type is shown in **Fig. 5**. Visual inspection does not reveal any obvious differences between the stellar types, except that the predominant constraint on the desert region arises from G-type stars.

Any statistically significant differences among the stellar subsamples, as well as stringent constraints on the desert region will be indentified once occurence rates have been calculated in the lifetime-integrated X-ray flux parameter space. We are adopting a methodology similar to that of Howard et al. 2012 in calculating planet occurence rates within cells, wherein the number of planet candidates within a cell are divided by the number of stars for which a planet detection is feasible. Our occurence rates will be reported as a function of planet radius and lifetime-integrated X-ray flux, rather than the orbital period used in Howard et al. 2012 and Dressing and Charbonneau 2013.

The calculation of occurence rates requires a sample for which detection by *Kepler* is considered complete. We adopt criteria similar to that of Wolfgang and Lopez 2015 who investigated the composition distribution of sub-Neptunes in the *Kepler* data. Specifically, using the Wolfgang and Lopez 2015 cuts such that the *Kepler* planets have $R_\oplus > 1.2$ and host star radii $R_* < 1.2$, while modifying the orbital period cut to be $P \lesssim 10$ days where photoevaporation is important. Our restriction to shorter orbital periods than the $P \lesssim 25$ days of Wolfgang and Lopez 2015 enables us to consider noisier stars (in terms of Combined Differential Photometric Precision, CDPP) with CDPP $\lesssim 200$ ppm (compared to < 100 ppm in Wolfgang and Lopez 2015).

With a sample for which *Kepler* detections are complete, we will calculate occurence as a function of planetary radius and lifetime-integrated X-ray flux. Specifically, we will subdivide the complete sample into two radii bins: $1.2 - 1.6\ R_{\oplus}$ and $1.6 - 4\ R_{\oplus}$, consistent with rocky planets for the former and those with gaseous envelopes for the latter (Rogers, 2015). Occurence as a function of lifetime-integrated X-ray flux will be calculated for these two radii bins. Any statistical significant differences, particularly a dearth of planets with gaseous envelopes for lifetime-integrated X-ray fluxes $\gtrsim 4 \times 10^{21}\ erg/cm^2$ anticipated from our current analysis, and any corresponding enhancement in occurence in the rocky planet bin, would suggest an evolution of very close-in sub-Neptunes initially formed with H/He envelopes to rocky planets through photoevaporation.

4 Conclusions

We have developed a framework for calculating lifetime-integrated X-ray fluxes for planets in the *Kepler* database. We find that for an age of 5 Gyr and at a semi-major axis of 0.01 AU, the lifetime-integrated X-ray flux varies by only an order of magnitude for stars with $0.3 < M_{\odot} < 1.598$. Upon calculation of lifetime-integrated X-ray fluxes for all confirmed *Kepler* planets, we note a dearth of planets with lifetime-integrated X-ray fluxes $\gtrsim 4 \times 10^{21}\ erg/cm^2$, with evidence that this drop-off is more pronounced for the lifetime-integrated X-ray flux parameter space (which ties directly to the photoevaporation process) when compared to the present-day bolometric flux examined in previous studies.

The relative uncertainties in the *Kepler*-derived stellar masses and planetary radii are large (a mean 1σ relative error of 30% for the latter). Our calculation of planet occurence rates in the lifetime-integrated X-ray flux parameter space will place more robust bounds on the desert region, as well as make apparent any variations in the desert region for different stellar spectral types. Finally, adding the first 104 confirmed planets from the K2 mission will also facillitate the comparison among stellar spectral types, particularly in increasing the sample size of the planets around K and M-type stars.

References

Baraffe, I., Chabrier, G., Allard, F., Hauschildt, P. H., 1998. Evolutionary models for solar metallicity low-mass stars : mass-magnitude relationships and color-magnitude diagrams. Astronomy and Astrophysics 337, 403–412.

Crossfield, I. J. M., Ciardi, D. R., Petigura, E. A., Sinukoff, E., Joshua, E., Howard, A. W., Beichman, C. A., Isaacson, H., Courtney, D., Christiansen, J. L., Fulton, B. J., Lépine, S., Weiss, L., Hirsch, L., Livingston, J., Baranec, C., Law, N. M., Riddle, R., Howell, S. B., Horch, E., Everett, M., Teske, J., Arturo, O., Obermeier, C., Benneke, B., Scott, N., Deacon, N., Kimberly, M., 2016. 197 Candidates and 104 Validated Planets in K2's First Five Fields. arXiv.

Dotter, A., Chaboyer, B., Jevremovic, D., Kostov, V., Baron, E., Ferguson, J. W., 2008. The Dartmouth Stellar Evolution Database. \Apjs 178 (2007), 37.
URL `http://arxiv.org/abs/0804.4473`

Dressing, C. D., Charbonneau, D., 2013. The Occurrence Rate of Small Planets Around Small Stars. The Astrophysical Journal 767 (1), 95.
URL `http://stacks.iop.org/0004-637X/767/i=1/a=95\nhttp://stacks.iop.org/0004-637X/767/i=1/a=95?ke`

Fressin, F., Torres, G., Charbonneau, D., Bryson, S. T., Christiansen, J., Dressing, C. D., Jenkins, J. M., Walkowicz, L. M., Batalha, N. M., 2013. THE FALSE POSITIVE RATE OF KEPLER AND THE OCCURRENCE OF PLANETS. The Astrophysical Journal 766 (81), 1–20.

Howard, A. W., Marcy, G. W., Bryson, S. T., Jenkins, J. M., Rowe, J. F., Batalha, N. M., Borucki, W. J., Koch, D. G., Dunham, E. W., Iii, T. N. G., Cleve, J. V., Cochran, W. D., Latham, D. W., Lissauer, J. J., Torres, G., Brown, T. M., Gilliland, R. L., Buchhave, L. A., Caldwell,

D. A., Christensen-dalsgaard, J., Ciardi, D., Fressin, F., Haas, M. R., Howell, S. B., Kjeldsen, H., Seager, S., Rogers, L., Sasselov, D. D., Steffen, J. H., Basri, G. S., Charbonneau, D., Christiansen, J., Clarke, B., Dupree, A., Fabrycky, D. C., Fischer, D. A., Ford, E. B., Fortney, J. J., Tarter, J., Girouard, F. R., Holman, M. J., Johnson, J. A., Klaus, T. C., Machalek, P., Moorhead, A. V., Morehead, R. C., Ragozzine, D., Tenenbaum, P., Twicken, J. D., Quinn, S. N., Isaacson, H., Shporer, A., Lucas, P. W., Walkowicz, L. M., Welsh, W. F., Boss, A., Devore, E., Gould, A., Smith, J. C., Morris, R. L., Prsa, A., Morton, T. D., Still, M., Thompson, S. E., Mullally, F., Endl, M., Macqueen, P. J., 2012. PLANET OCCURRENCE WITHIN 0 . 25 AU OF SOLAR-TYPE STARS FROM KEPLER. The Astrophysical Journal Supplement Series 201 (15), 1–20.

Huber, D., Aguirre, V. S., Matthews, J. M., Pinsonneault, M. H., Gaidos, E., Garc, R. A., Basu, S., Bedding, T. R., Chaplin, W. J., Demory, B.-o., Fleming, S. W., Guo, Z., Mann, A. W., Rowe, J. F., Serenelli, A. M., Smith, M. A., Stello, D., 2014. REVISED STELLAR PROPERTIES OF KEPLER TARGETS FOR THE QUARTER 1 − 16 TRANSIT DETECTION RUN. The Astrophysical Journal Supplement Series 211 (2), 1–18.

Jackson, A. P., Davis, T. A., Wheatley, P. J., 2012. The coronal X-ray − age relation and its implications for the evaporation of exoplanets. Monthly Notices of the Royal Astronomical Society 422, 2024–2043.

Lecavelier Des Etangs, A., 2007. A diagram to determine the evaporation status of extrasolar planets. Astronomy and Astrophysics 461, 1185.
URL `http://adsabs.harvard.edu/cgi-bin/nph-data_query?bibcode=2007A%2526A...461.1185L&link_type=ABS`

Lopez, E. D., Fortney, J. J., 2014. UNDERSTANDING THE MASS – RADIUS RELATION FOR SUB-NEPTUNES : RADIUS AS A PROXY FOR COMPOSITION. The Astrophysical Journal 729 (1), 1–17.

Lopez, E. D., Fortney, J. J., Miller, N., 2012. HOW THERMAL EVOLUTION AND MASS-LOSS

SCULPT POPULATIONS OF SUPER-EARTHS AND SUB-NEPTUNES : APPLICATION TO THE KEPLER-11 SYSTEM AND BEYOND. The Astrophysical Journal 761 (59), 1–13.

Lundkvist, M. S., Kjeldsen, H., Albrecht, S., Davies, G. R., Basu, S., Huber, D., Justesen, A. B., Karoff, C., Aguirre, V. S., Eylen, V. V., Vang, C., Arentoft, T., Barclay, T., Bedding, T. R., Campante, T. L., Chaplin, W. J., Elsworth, Y. P., Gilliland, R. L., Handberg, R., Hekker, S., 2016. Hot super-Earths stripped by their host stars. Nature Communications 7, 1–8.
URL http://dx.doi.org/10.1038/ncomms11201

Morton, T. D., Bryson, S. T., Coughlin, J. L., Rowe, J. F., Ravichandran, G., Petigura, E. A., Haas, M. R., Batalha, N. M., 2016. FALSE POSITIVE PROBABILITIES FOR ALL KEPLER OBJECTS OF INTEREST : 1284 NEWLY VALIDATED PLANETS AND 428 LIKELY FALSE POSITIVES. The Astrophysical Journal 822 (2), 1–15.
URL http://dx.doi.org/10.3847/0004-637X/822/2/86

Murray-clay, R. A., Chiang, E. I., Murray, N., 2009. ATMOSPHERIC ESCAPE FROM HOT JUPITERS. The Astrophysical Journal 693, 23–42.

Owen, J. E., Jackson, A. P., 2012. Planetary evaporation by UV and X-ray radiation : basic hydrodynamics 1 I N T RO D U C T I O N 2 H E AT I N G M E C H A N I S M. Monthly Notices of the Royal Astronomical Society 425, 2931–2947.

Owen, J. E., Wu, Y., 2013. KEPLER PLANETS : A TALE OF EVAPORATION. The Astrophysical Journal 775 (105), 1–12.

Pecaut, M. J., Mamajek, E. E., 2013. Intrinsic Colors, Temperatures, and Bolometric Corrections of Pre-Main-Sequence Stars. The Astrophysical Journal Supplement Series 208 (1), 9.
URL http://stacks.iop.org/0067-0049/208/i=1/a=9?key=crossref.40637725e05e58390e6b2c1741c9f4ac

Petigura, E. A., Marcy, G. W., Howard, A. W., 2013. A plateau in the planet population below twice the size of earth 1. The Astrophysical Journal 770 (69), 1–21.

Rogers, L. A., 2015. MOST 1.6 EARTH-RADIUS PLANETS ARE NOT ROCKY. The Astrophysical Journal 801 (41), 1–13.
URL http://dx.doi.org/10.1088/0004-637X/801/1/41

Sanchis-Ojeda, R., Rappaport, S., Winn, J. N., Kotson, M. C., Levine, A., Mellah, I. E., 2014. A STUDY OF THE SHORTEST-PERIOD PLANETS FOUND WITH KEPLER. The Astrophysical Journal 878 (47), 1–18.

Sanz-Forcada, J., Micela, G., Ribas, I., Pollock, A. M. T., Eiroa, C., Velasco, A., Solano, E., Osservatorio, I., Vaiana, P. G. S., Parlamento, P., 2011. Estimation of the XUV radiation onto close planets and their evaporation. Astronomy and Astrophysics 532 (A6), 1–18.

Shkolnik, E., Barman, T., 2014. HAZMAT . I . THE EVOLUTION OF FAR-UV AND NEAR-UV EMISSION FROM EARLY M STARS. The Astrophysical Journal 148 (64), 1–14.

Silva Aguirre, V., Davies, G. R., Basu, S., Christensen-Dalsgaard, J., Creevey, O., Metcalfe, T. S., Bedding, T. R., Casagrande, L., Handberg, R., Lund, M. N., Nissen, P. E., Chaplin, W. J., Huber, D., Serenelli, A. M., Stello, D., Van Eylen, V., Campante, T. L., Elsworth, Y., Gilliland, R. L., Hekker, S., Karoff, C., Kawaler, S. D., Kjeldsen, H., Lundkvist, M. S., 2015. Ages and fundamental properties of Kepler exoplanet host stars from asteroseismology. Monthly Notices of the Royal Astronomical Society 452 (2), 2127–2148.

Weiss, L. M., Marcy, G. W., Rowe, J. F., Howard, A. W., Isaacson, H., Fortney, J. J., Miller, N., Demory, B.-o., Fischer, D. A., Adams, E. R., Dupree, A. K., Howell, S. B., Kolbl, R., Johnson, J. A., Horch, E. P., Everett, M. E., Fabrycky, D. C., Seager, S., 2013. THE MASS OF KOI-94d AND A RELATION FOR PLANET RADIUS , MASS , AND INCIDENT FLUX. The Astrophysical Journal 768 (14), 1–19.

Wolfgang, A., Lopez, E., 2015. How Rocky Are They? the Composition Distribution of Kepler 'S Sub-Neptune Planet Candidates Within 0.15 Au. The Astrophysical Journal 806 (2), 183.
URL http://stacks.iop.org/0004-637X/806/i=2/a=183?key=crossref.5cf17c111664baf03c7862f15219dfb2

Figures

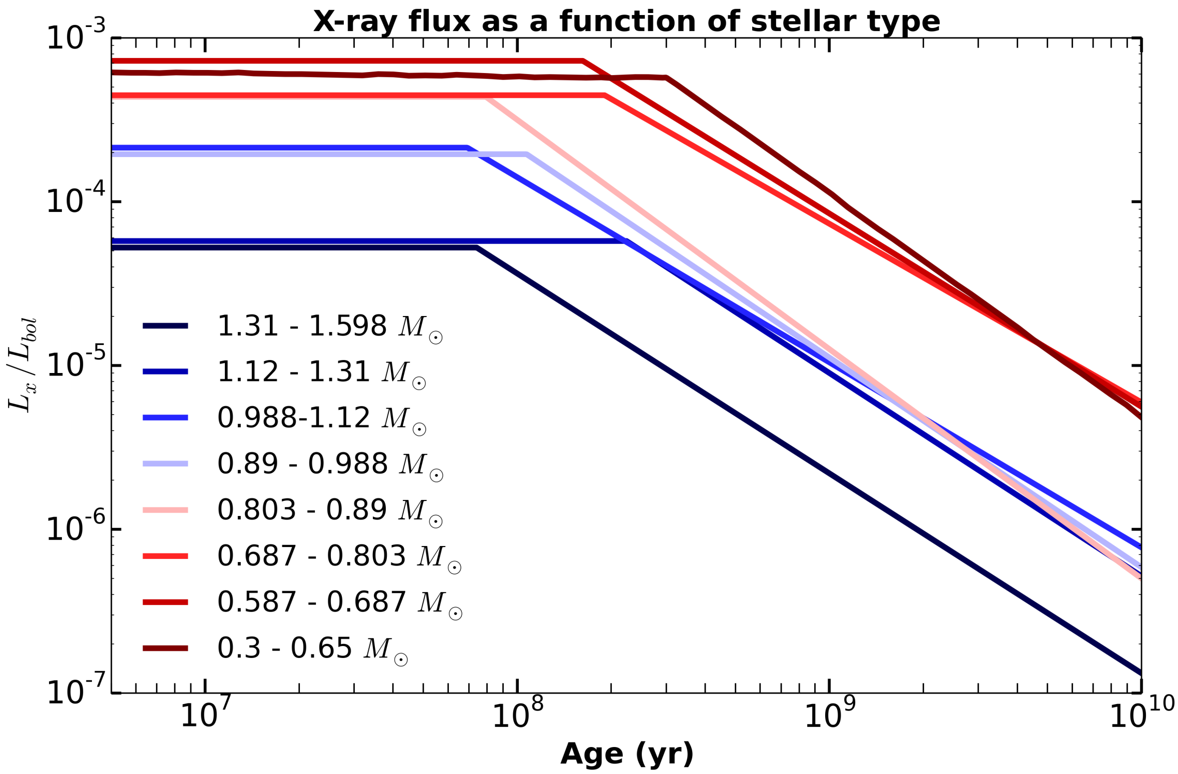

Fig. 1. The evolution of the X-ray to bolometric luminosity ratio as a function of stellar age, for stars with 0.3 $< M_\odot <$ 1.598. The evolutionary track for stars with 0.3 $< M_\odot <$ 0.65 is taken from Shkolnik and Barman 2014, while the relations for stars with $M_\odot >$ 0.587 are taken from Jackson et al. 2012.

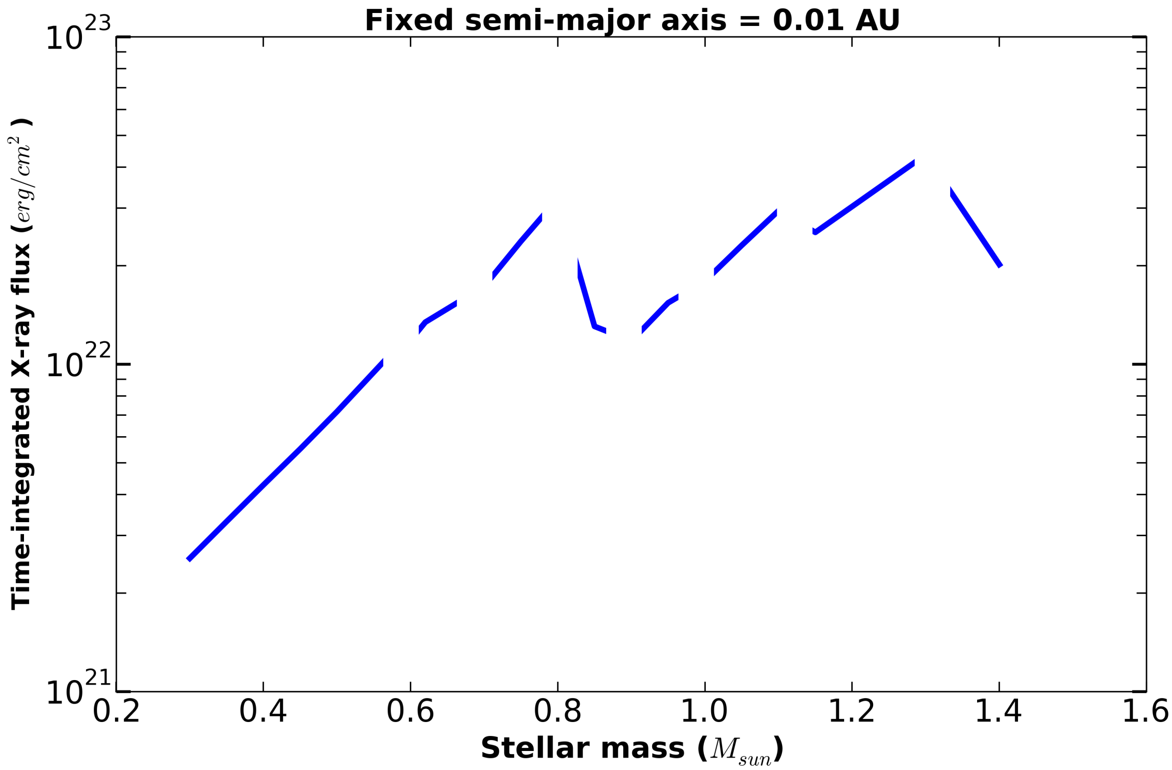

Fig. 2. The lifetime-integrated X-ray flux as a function of stellar mass. This has been calculated for a planet with a semi-major axis of 0.01 AU orbiting a star of age 5 Gyr. The separate lines represent the different bins in stellar spectral type from the Jackson et al. 2012 and Shkolnik and Barman 2014 X-ray luminosity evolution relations. The trends within each line are solely the result of bolometric luminosity variations as a function of stellar mass, as taken from the Baraffe et al. 1998 stellar evolution tracks.

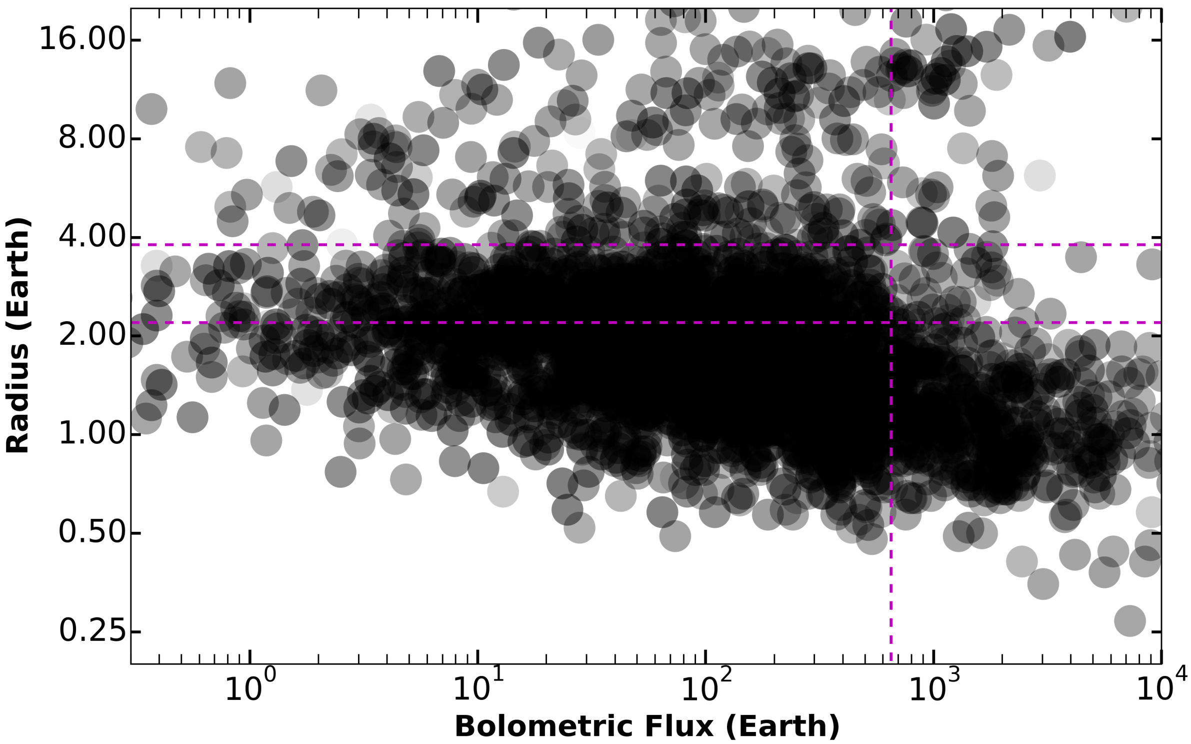

Fig. 3. The full sample of *Kepler* planets as confirmed by the uniform false-postive probability analysis of Morton et al. 2016, using the Q1-Q17 DR 24 KOI catalog, in the parameter space of planetary radius vs present-day bolometric flux. The precision of the measurements for a given planet is indicated by the shading, such that high precision planets are dark and low precision planets are light-colored. As such, dark regions indicate areas of higher planet density, either from high precision measurements, or predominantly, from multiple planets with similar radii and bolometric fluxes. The desert region reported by Lundkvist et al. 2016 is the rectangular region bounded by dashed purple lines with a bolometric flux ¿ 650 $F_{\oplus}$ and radii between 2.2 and 3.8 $R_{\oplus}$.

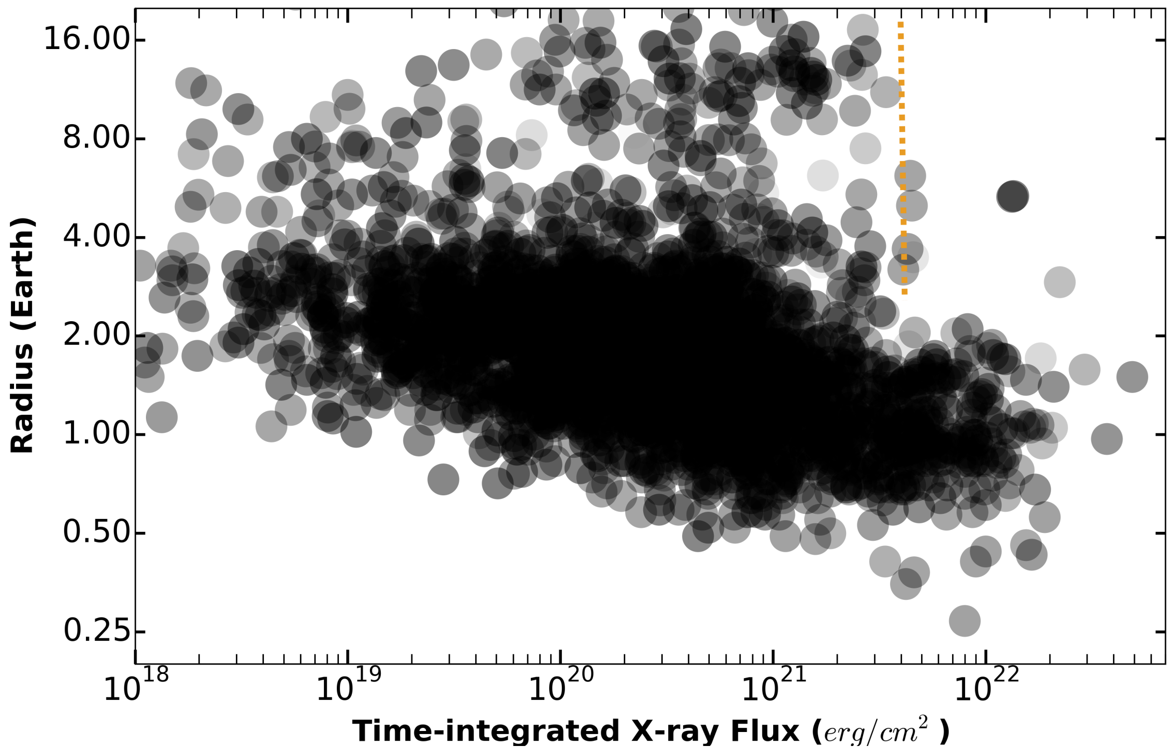

Fig. 4. The same sample of confirmed *Kepler* planets as Fig. 3, but in the parameter space of planetary radius vs lifetime-integrated X-ray flux assuming stellar ages of 5 Gyr for the full *Kepler* sample. The line at 4×10^{21} erg/cm^2 indicates the inferred lifetime-integrated X-ray flux bound for the desert region. The plotting conventions are the same as that of Fig. 3.

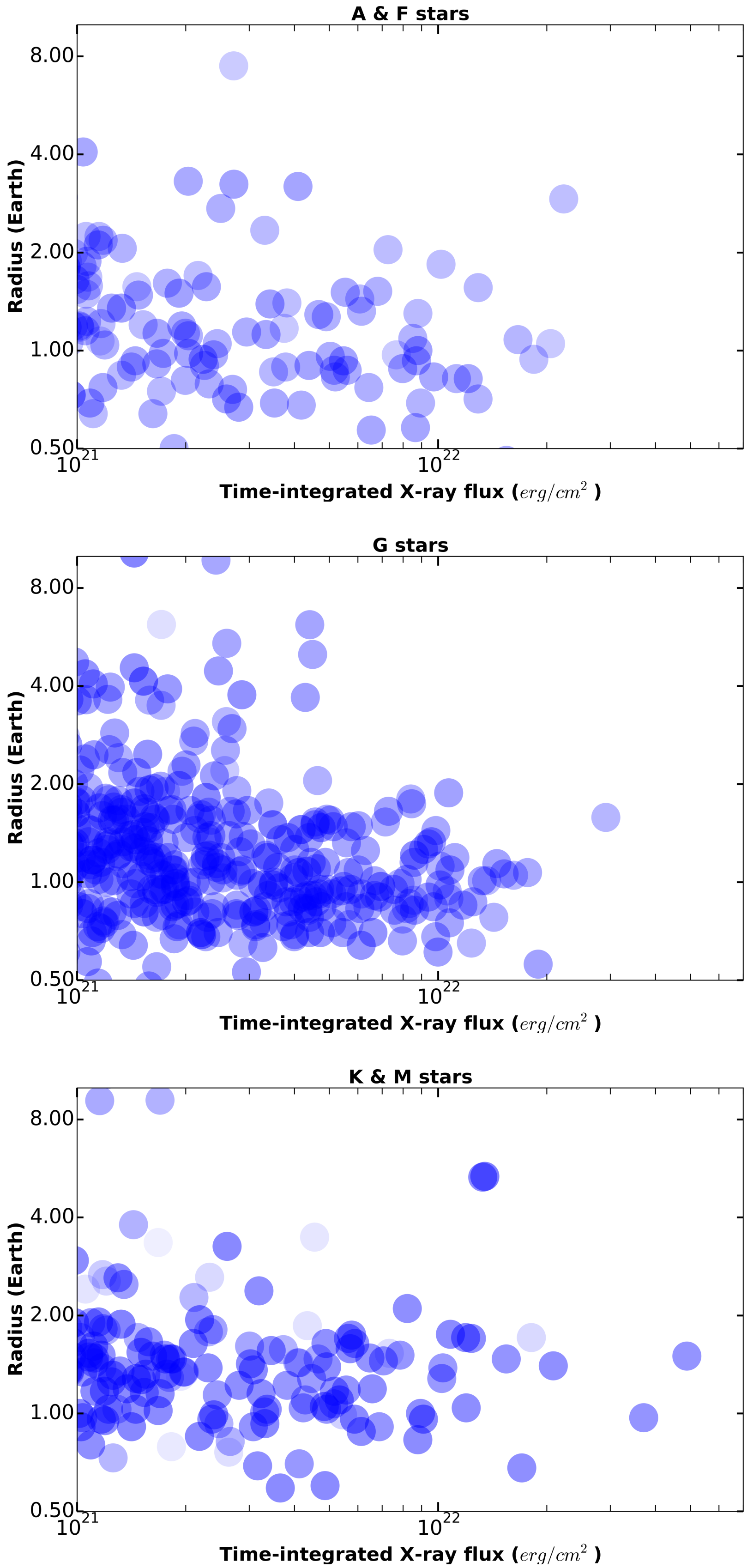

Fig. 5. The same sample of confirmed *Kepler* planets and parameter space shown in Fig. 4, but subdivided by stellar spectral type.